

A COUPLED-MODE MODEL FOR THE PROPAGATION OF MILLIMETER ELECTROMAGNETIC WAVES IN A TROPOSPHERIC DUCT OVERLYING A RANDOMLY ROUGH SEA SURFACE

A coupled-mode model was developed to address the problem of long-range propagation of acoustic waves in an oceanic surface duct. The model presents an exact solution of the wave equation for an inhomogeneous, oceanic waveguide bounded by a randomly rough sea surface. It includes full-mode coupling and accounts for both the forward propagating wave and the backscattered wave. This article demonstrates that the acoustic coupled-mode model can be used to describe millimeter-electromagnetic-wave propagation and scattering in a tropospheric duct overlying a randomly rough sea surface.

INTRODUCTION

Rough-surface scattering models can be divided into two groups. The first consists of models with a rough surface overlying a homogeneous medium that extends to infinity. The second can handle the multiple scattering of a wave propagating along a waveguide.

In the first group, a point source is located either a finite distance from the surface or at infinity, in which case the incident waves are planar. Common to all the models is a single act of scattering from the rough surface. Once the incident wave interacts with the rough surface, it propagates to infinity, never again interacting with the surface. Slight perturbations in the boundary can produce only slight distortions in the scattered field.

In the second group, the medium can be either homogeneous or refracting. The source is still modeled as a point source, but now the wave propagating along the waveguide interacts repeatedly with one or both rough surfaces. Hence, the field at the receiver is the phased sum of the waves scattered multiply by the irregularities distributed along the entire waveguide. Even very slight boundary perturbations can give rise to considerable distortions in the scattered field by virtue of the accumulated effects of repeated scatterings. This is the situation in naturally occurring waveguides such as the ocean (for acoustic waves) and the troposphere (for electromagnetic waves). The coupled-mode model falls into the second category.

The term "coupled modes" arises from the following considerations. We are seeking a solution of the wave equation for a wave that is confined to a waveguide. The waveguide is bounded in only one space coordinate (the z coordinate) by two surfaces. It is open to infinity in the x and y directions. Because the problem is bounded in the z direction, the wave functions characterizing that direction are a discrete set of complete, orthonormal eigenfunctions. Each eigenfunction, called a mode, describes the characteristic vibrations of the waveguide in

the z direction. If the two surfaces bounding the waveguide are smooth parallel planes, the energy that starts out initially in a mode remains unchanged in that mode as the wave propagates along the waveguide. When the surfaces are rough, energy can be transferred from mode to mode as the wave propagates. Hence the modes are "coupled" to each other.

Issues in passive and active ocean acoustics motivated the development of the coupled-mode model¹ that we will discuss. Passive acoustic systems detect sound energy radiated by a target. Active systems transmit a pulse and detect its echo from a target. In active systems there is the additional problem of reverberation—unwanted sound energy that is scattered back to the receiver from the rough boundaries and that masks the target return. The coupled-mode model describes the forward propagation and scattering of the acoustic pulse as well as the reverberation.

Rough-surface scattering effects are enhanced by the presence of surface ducts in the ocean. In certain areas of the world's oceans, an isothermal layer is created and maintained beneath the sea surface by wind mixing; the layer can be hundreds of meters thick in some areas. The sound velocity in the layer increases with depth because of pressure. If a source is placed in the layer, a significant amount of energy can become trapped there; the exact amount depends on frequency, layer thickness, and the sound velocity gradients in and directly beneath the layer. The energy propagates along the duct by repeated refractions and surface reflections. Because the wave traveling along the duct interacts many times with the surface, it is necessary to have a model that includes rough-surface scattering effects. Also, because variations in duct thickness and in the sound velocity gradient can have a profound effect on the transmission of energy along the duct, we must be able to allow for variation of the sound speed profile with horizontal range.

Two models were developed at APL to take into account the environmental conditions mentioned above. The first solved the problem of a cylindrically symmetric oceanic waveguide with both horizontal and vertical variations in the refractive index and a single realization of a randomly rough sea surface; the model's geometry is shown in Fig. 1a. The main limitation of this model is that the assumption of cylindrical symmetry precludes any scattering out of the vertical plane. In the second (Cartesian) model, the limitation of cylindrical symmetry was removed, and a sea running in one direction was treated; the geometry of this model is shown in Fig. 1b. Both models assume a point source, include full-mode coupling, and account for the forward and backscattered waves. Thus, both yield an exact solution of the wave equation for a randomly rough sea surface. Scattering out of the vertical plane is allowed in the Cartesian model because a point source is used.

Because these models use a single realization of a random surface, statistics for the scattered field can be obtained by means of a Monte Carlo simulation. Statistics can be generated by using different realizations of the random surface at a fixed time. One can also allow the surface to develop in time for a fixed choice of random parameters, yielding the Doppler spectrum for the surface.

The theory for both models is presented in detail in Ref. 2; the numerical algorithm that was used to integrate the coupled differential equations is discussed in Ref. 3. A computer code exists only for the cylindrical model; it does not contain a variation of the refractive index with horizontal range. Our next task is to include horizontal range variations in the computer code, since they are already accounted for in the theory. We will discuss only the cylindrical model here.

The coupled-mode model has been successfully applied to acoustic propagation in an oceanic waveguide; we have begun to investigate the possibility of applying it to describe millimeter-electromagnetic-wave propagation in a tropospheric duct bounded by a rough sea surface. At these frequencies we must include scattering from capillary waves. Because of the boundary conditions already built into the acoustic model, only one type of electromagnetic propagation can be addressed: the case of a horizontally polarized electric wave scattering off a sea of infinite conductivity. This article is not intended to give a definitive answer to millimeter-electromagnetic-wave scattering from a rough surface, since we have just begun to address the problem. Instead, it demonstrates that the acoustic coupled-mode model can be used to describe millimeter-electromagnetic-wave propagation and scattering from a rough sea surface.

COUPLED-MODE THEORY

The separation of variables is a powerful technique for solving partial differential equations. However, there are only 11 three-dimensional coordinate systems in which the wave equation is separable.⁴ The technique of separation of variables can be used only if in one system each boundary of the medium coincides with a coordinate sur-

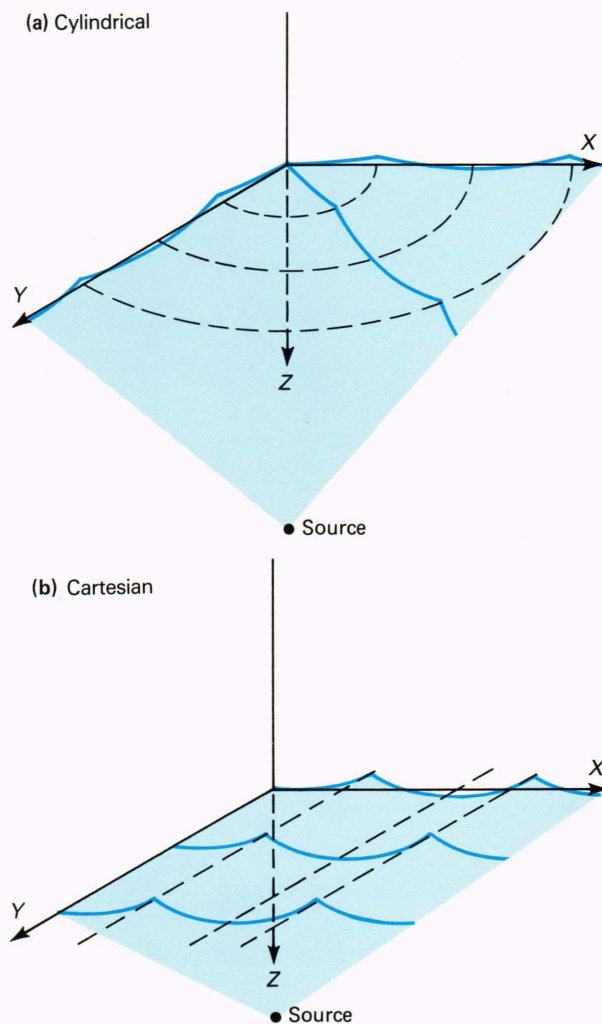


Figure 1—Examples of realization of the sea surface in two geometries.

face and, further, if the refractive index is additively separable in the coordinates.

One method of solving nonseparable problems is the technique of coupled modes in which the partial differential wave equation is replaced by a system of coupled, ordinary differential equations. The coupled differential equations give an exact and rigorous description of wave propagation for nonseparable problems. The method has existed at least since 1927 when Born and Oppenheimer⁵ applied it to the Schrödinger wave equation.

The description of mode coupling is not unique. There are different ways of obtaining a system of coupled differential equations.⁶ We will consider only one method in this article, the method of local normal modes. What follows is a brief summary of the theory; a detailed treatment can be found in Ref. 2.

We consider the problem of a point source located at $r = 0$ and $z = z_s$ in a cylindrically symmetric oceanic waveguide. The coordinate system in relation to the waveguide is shown in Fig. 2. The bottom of the waveguide is bounded by the sea surface, which is given as a function of range r and time t as

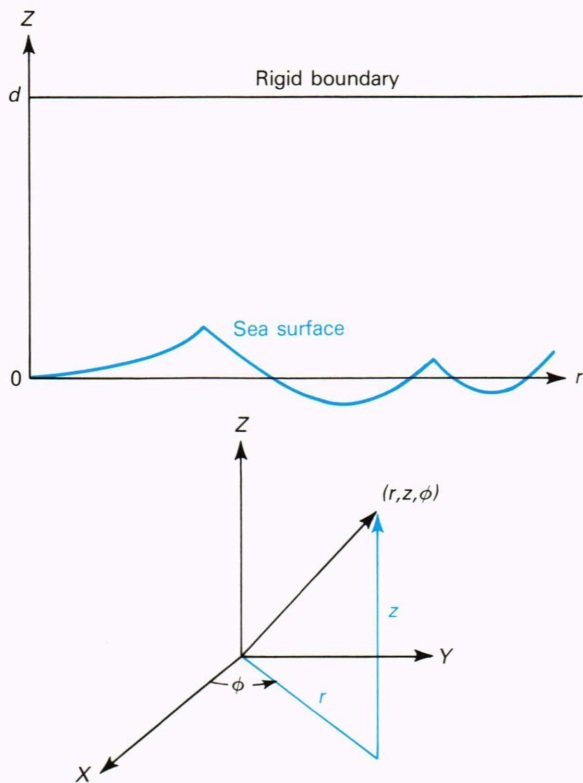


Figure 2—Coordinate geometry for the cylindrical waveguide.

$$z = s(r,t) . \tag{1}$$

The top of the waveguide is bounded by a flat, rigid surface. As stated above, for this first derivation of an electromagnetic propagation model, the boundary conditions were not changed from those of the acoustic model. Future development of this theory will lead to more realistic boundary conditions at the top of the atmosphere, such as an infinite halfspace above the sea surface, so that the electromagnetic radiation can escape to outer space. However, that condition can be approximated with the model we have if we put a highly absorbing layer just beneath the rigid boundary. Then any radiation that reaches that height is removed from the waveguide as if it had escaped to outer space.

The wave velocity $v(r,z)$ in the waveguide can be a function of both range r and height z . The wave equation that governs the electric field away from the source is

$$\nabla^2 \varepsilon - n^2 \frac{\partial^2 \varepsilon}{\partial t^2} = 0 . \tag{2}$$

In Eq. 2, $\varepsilon(r,z,t)$ is the ϕ -component of the electric field vector, and $n(r,z)$ is the refractive index of the medium, defined by

$$n(r,z) = c/v(r,z) , \tag{3}$$

where c is the speed of light in vacuum.

Let us assume that we are dealing with an electric wave of a single angular frequency ω . Then we can write

$$\varepsilon(r,z,t) = E(r,z)e^{-i\omega t} , \tag{4}$$

where $E(r,z)$ is the portion of the electric field that is independent of time. Using Eq. 4, we can write Eq. 2 in cylindrical coordinates as

$$\frac{\partial^2 E}{\partial r^2} + \frac{1}{r} \frac{\partial E}{\partial r} + \frac{\partial^2 E}{\partial z^2} + k^2(r,z)E = 0 , \tag{5}$$

where

$$k(r,z) = \omega n(r,z) . \tag{6}$$

Derivatives with respect to ϕ do not appear in Eq. 5, because of the assumption of cylindrical symmetry.

Equation 5 is called the Helmholtz equation or the space part of the wave equation. It is exact when the boundaries of the medium in which the wave is propagating are independent of time. But we want to consider a time-varying sea surface, which would normally mean that instead of solving the Helmholtz equation (an elliptic partial differential equation) we would have to solve the full-wave equation, Eq. 2, which is a hyperbolic partial differential equation. The numerical solution of the full hyperbolic problem with a rough, time-varying boundary is impractical, however. Fortunately, since the frequencies of the moving ocean surface that control the scattering process are much lower than the electromagnetic frequency in all cases of interest to us, we can invoke the narrowband approximation to the wave equation, expressed mathematically by

$$\frac{\partial^2 \varepsilon}{\partial t^2} \approx -\omega^2 \varepsilon . \tag{7}$$

This approximation is discussed in detail in the papers by Fortuin⁷ and Labianca and Harper.⁸ It is equivalent to solving the Helmholtz equation for a time-dependent boundary. Instead of Eq. 4, however, we now have

$$\varepsilon(r,z,t) = E(r,z,t)e^{-i\omega t} , \tag{8}$$

where $E(r,z,t)$ becomes a slowly varying function of time through the application of the boundary conditions.

Fourier-transforming the solutions $\varepsilon(r,z,t_i)$ obtained at a set of discrete times t_i yields the Doppler frequency spectrum at the point (r,z) .

We postulate a solution of the form

$$E = \sum_{n=1} \Phi_n(r)\Psi_n(r,z) . \tag{9}$$

Note that in contrast to the usual normal-mode solution, which uses separation of variables, the eigenfunctions Ψ_n depend on the range as well as the height. Consequently, they are called “local” normal modes. For the range-independent problem, the modes Ψ_n are independent of range and hence form a “global” solution; that is, a given mode is supported unchanged along the entire length of the waveguide.

We also postulate that the local eigenfunctions Ψ_n satisfy the partial differential equation

$$\frac{\partial^2 \Psi_n}{\partial z^2} + [k^2(r, z) - \kappa_n^2(r)] \Psi_n = 0 \quad (10a)$$

and the following boundary conditions: on the sea surface,

$$E[r, s(r, t), t] = 0, \quad (10b)$$

and on the rigid upper boundary,

$$\left[\frac{\partial E(r, z, t)}{\partial z} \right]_{z=d} = 0, \quad (10c)$$

where d is the thickness of the waveguide. The validity of the postulates given by Eqs. 9 and 10 must be confirmed by experimental measurement.

The variable $\kappa_n(r)$ is the “local” eigenvalue of the problem. It is determined at each point of the waveguide by the wave velocity profile and the boundary conditions. In the usual range-independent normal-mode solutions, the eigenvalues are constants, independent of the horizontal range.

The only difference in mathematical structure between Eq. 10 for the local modes and the corresponding equation for the range-independent case is that the former is a partial differential equation and the latter is an ordinary differential equation. A partial differential equation is necessary here because we are postulating that the local modes can now be a function of range as well as height.

It can be shown that the eigenfunction solutions Ψ_n of Eq. 10, subject to the boundary conditions, form a complete orthonormal system at each range point r . The orthonormality condition is

$$\int_s^d \Psi_n(r, z) \Psi_m(r, z) dz = \delta_{nm}. \quad (11)$$

Thus, the modal structure of a range-dependent waveguide varies from point to point along the waveguide. At each point the modal structure depends on the frequency, the boundary conditions, the wave velocity profile, and the thickness of the waveguide, and the modal structure can vary along the waveguide because of variations in the latter two quantities. Equation 11 implies that the local modes must be renormalized at each point.

That the modes are different at each point along the waveguide implies the existence of a mode-coupling process that is best expressed in terms of waves propagating in the forward and backward radial direction rather than in terms of the total field $\Phi_m(r)$. Consequently, we let

$$\Phi_m(r) = a_m^+(r) + a_m^-(r), \quad (12)$$

where $a_m^+(r)$ is the forward-propagating wave and $a_m^-(r)$ is the backward-propagating, or backscattered, wave. The application of the boundary conditions determines whether a function represents the forward or the backscattered wave. The boundary conditions will be discussed later in this section.

The coupled equations that determine the radial propagating waves are

$$\begin{aligned} \frac{da_m^+}{dr} - \left(ik_m - \frac{1}{2r} \right) a_m^+ \\ = \sum_{n=1}^{\infty} B_{m^+ n^+} a_n^+ + \sum_{n=1}^{\infty} B_{m^+ n^-} a_n^-, \end{aligned} \quad (13)$$

$$\begin{aligned} \frac{da_m^-}{dr} + \left(ik_m + \frac{1}{2r} \right) a_m^- \\ = \sum_{n=1}^{\infty} B_{m^- n^+} a_n^+ + \sum_{n=1}^{\infty} B_{m^- n^-} a_n^-. \end{aligned}$$

Here the coupling coefficients are given by

$$\begin{aligned} B_{m^+ n^+} &= \frac{-1}{2\kappa_m} \left[(\kappa_n + \kappa_m) B_{mn} + \delta_{mn} \frac{d\kappa_n}{dr} \right], \\ B_{m^+ n^-} &= \frac{1}{2\kappa_m} \left[(\kappa_n - \kappa_m) B_{mn} + \delta_{mn} \frac{d\kappa_n}{dr} \right], \\ B_{m^- n^+} &= B_{m^+ n^-}, \\ B_{m^- n^-} &= B_{m^+ n^+}, \end{aligned} \quad (14)$$

$$B_{mn} = S_{mn} + N_{mn} \quad (m \neq n),$$

$$B_{nn} = 0,$$

where for $m \neq n$,

$$S_{mn} = \frac{1}{(\kappa_m^2 - \kappa_n^2)} \left(\frac{\partial \Psi_m}{\partial z} \frac{\partial \Psi_n}{\partial z} \frac{ds}{dr} \right)_{z=s}$$

and

$$N_{mn} = \frac{-2\omega^2}{(\kappa_m^2 - \kappa_n^2)} \int_s^d n \frac{\partial n}{\partial r} \Psi_m \Psi_n dz .$$

First consider the coupling coefficients S_{mn} , which control the exchange of energy resulting from the rough sea surface. We see that they are inversely proportional to the difference of the squares of the modal wave numbers κ_n , so that coupling is strongest for two neighboring modes. Since the squares of the modal wave numbers appear, S_{mn} feeds the same power into both forward and backward-traveling waves at a given range point. Whether this power builds up in either the forward or the backscattered waves depends on the phase relationship of the incremental amounts of power fed to the wave at other points. A wave builds up only if the incremental contributions at all points along the waveguide add up in phase. We note that S_{mn} is proportional to the slope ($\partial \Psi_n / \partial z$) of the wave function at the sea surface, a very reasonable result. One way to look at this is to consider the ray equivalent⁹ for a mode. As the order of the mode increases, the slope of the wave function at the surface and therefore the strength of the coupling increase. But as the order of the mode increases, the ray equivalent strikes the surface at larger and larger grazing angles, and we would expect more pronounced scattering. Finally, we see that S_{mn} is proportional to the slope of the sea surface.

The second term N_{mn} in the expression for the coupling coefficient B_{mn} is associated with mode coupling arising from horizontal gradients ($\partial n / \partial r$) in the index of refraction $n(r, z)$.

We confine the range-dependent properties of the waveguide to an interval $R_0 < r < R_1$; that is, the surface is assumed to be flat, and the wave velocity depends only on height outside this region. The only requirement we put on R_0 is that $\kappa_m R_0 \gg 1$. This is not a limitation of the theory, but it does simplify the numerical code. The value for R_1 can be hundreds of nautical miles. The boundary conditions on the variables a_n^+ and a_n^- are specified by their values at R_0 and R_1 , respectively. To satisfy the radiation condition at infinity, we assume that

$$a_n^-(R_1) = 0 . \quad (16)$$

Because the waveguide has no range-dependent properties from R_1 to infinity, an outgoing wave at infinity is guaranteed. The initial section of the waveguide ($0 < r < R_0$) is range-independent; therefore, a normal mode expansion of a point source is used to calculate $a_n^+(R_0)$.

A very common approximation applied to the coupled set of differential equations to make them numerically tractable is the adiabatic approximation in which

all coupling coefficients are neglected, thus uncoupling Eq. 13. However, the equations are still weakly range-dependent through the eigenvalues $\kappa_n(r)$. With this technique a weakly range-dependent environment can be treated quite simply. In this article the adiabatic approximation is not used, and full-mode coupling is always taken into account.

A MODEL FOR A TIME-VARYING, RANDOMLY ROUGH SEA SURFACE

It should be borne in mind that the propagation model is independent of any surface model and that any other model simulating a random sea surface could be used instead of the one described in this section. The model we will use was adapted by Harper and Labianca¹⁰ from a more general model proposed by Pierson.¹¹ The random surface is simulated by

$$z = s(r, t) = \sum_{j=1}^M h_j \cos(\Gamma_j r - \Omega_j' t + \gamma_j) , \quad (17)$$

where Ω_j' is the angular frequency ($\Omega_j' > 0$), taken to be a statistically independent, random variable, and Γ_j is the wave number. The dispersion relationship is

$$\Omega_j'^2 = g\Gamma_j + \frac{\tau\Gamma_j^3}{\rho} . \quad (18)$$

Here g is the acceleration due to gravity, ρ is the density of seawater, and τ is the surface tension. The phases γ_j are also taken to be statistically independent, random variables uniformly distributed between 0 and 2π . The amplitudes h_j are chosen in a deterministic manner described below. The process, Eq. 17, is ergodic with respect to its mean and autocorrelation function under a restriction on Ω_j' , which we shall describe.

Under the assumption that the power spectrum $P(\Omega')$ is band-limited, $\Omega_{\min} \leq \Omega' \leq \Omega_{\max}$, we define the equal intervals

$$\Delta\Omega = (1/M)(\Omega_{\max} - \Omega_{\min}) \quad (19)$$

and the discrete set of frequencies

$$\Omega_j = \Omega_{\min} + (j - 1/2)\Delta\Omega \quad (j = 1, \dots, M) . \quad (20)$$

The set of random frequencies Ω_j' is statistically independent of γ_j and is defined by

$$\Omega_j' = \Omega_j + \delta\Omega_j \quad (j = 1, \dots, M) , \quad (21)$$

where the $\delta\Omega_j$ are random variables uniformly distributed between $-\epsilon/2$ and $\epsilon/2$ with $\epsilon \ll \Delta\Omega$. This definition

ensures the ergodicity, in an approximate sense, of the simulated process $z = s(r, t)$ with respect to its correlation function.

The amplitudes h_j are determined according to the prescription

$$h_j^2 = 2P(\Omega_j') , \quad (22)$$

where $P(\Omega_j')$ is the power spectrum for the surface wave height.

Note that had we chosen the Ω_j' to be deterministic, say $\Omega_j' = \Omega_j$, the process $s(r, t)$ would be ergodic exactly with respect to its autocorrelation function. The main reason for requiring Ω_j' to have a small random part $\delta\Omega_j$ is to preclude the periodicity of $s(r, t)$ in time.

We will discuss only two wave-height spectra in this article: the Pierson-Moskowitz spectrum¹² and the Liu and Lin spectrum.¹³

The Pierson-Moskowitz spectrum holds in the angular frequency range $0 < \Omega' < 8.605/u$ and is given by

$$P(\Omega') = \frac{\alpha g^2}{\Omega'^5} \exp[-\beta(\Omega_0/\Omega')^4] , \quad (23)$$

where

$$\begin{aligned} \alpha &= 0.0081, \\ \beta &= 0.74, \\ \Omega_0 &= g/u, \\ u &= \text{wind speed (m/s)}. \end{aligned}$$

Toward the high-frequency end of the wind-wave spectrum, waves that are controlled partly or entirely by surface tension may be categorized as gravity-capillary or capillary waves, respectively. Although the demarcation between them is arbitrary, gravity-capillary waves are usually defined as those with wavelengths between 7 and 0.6 cm or a frequency between 5.0 and 48.5 Hz; capillary waves are those with wavelengths less than 0.6 cm. In this article we are interested in the capillary regime between 50 and 80 Hz. Consequently, we chose the Liu and Lin spectrum for capillary waves because their measurements were made with a laser displacement gauge, a nonintrusive sensor. The Liu and Lin spectrum is given by

$$P(\Omega') = (2\pi)^{7/3} \beta \gamma^{2/3} (\Omega')^{-7/3} , \quad (24)$$

where

$$\begin{aligned} \beta &= 2.73 \times 10^{-4} (u_0/c_m)^{9/4}, \\ \gamma &= \tau/\rho, \\ u_0 &= \text{friction velocity,} \end{aligned}$$

$$\begin{aligned} c_m &= \text{minimum phase speed of} \\ &\quad \text{the capillary wave,} \\ \tau &= \text{surface tension,} \\ \rho &= \text{density of water.} \end{aligned}$$

PROPAGATION IN A TROPOSPHERIC DUCT AT 3 GHz

For a discussion of the basic physical concepts governing microwave propagation in a tropospheric duct, we refer the reader to an excellent article by Ko, Sari, and Skura.¹⁴ In addition to discussing the basic features of microwave propagation in a duct, they also present a new propagation model, EMPE (Electromagnetic Parabolic Equation), based on the parabolic equation approximation to the full-wave equation. Essentially, the approximation replaces the Helmholtz equation—an elliptic partial differential equation—with a parabolic partial differential equation by neglecting a second derivative with respect to range. The method has the effect of simplifying the boundary conditions imposed on the range. A unique, stable solution exists for an elliptic partial differential equation when the field or its derivative is specified on a closed boundary. A boundary is closed if it completely surrounds the solution (even if part of the boundary is at infinity). A boundary is open if the boundary goes to infinity and no boundary conditions are imposed along the part at infinity. When the field or its derivative is specified on an open boundary for a parabolic equation, a unique stable solution exists in the positive direction (here, increasing range). This simplification in the boundary conditions permits easy numerical handling of problems in which the refractive index varies with horizontal range.

Physically, the parabolic approximation has two effects. First, it neglects backscattering.¹⁵ Second, McDaniel¹⁶ has shown that discrete modes are propagated with the correct amplitude and mode shapes but with errors in the phase velocities. The phase velocity for the n th mode v_n is ω/κ_n . Only one mode is propagated without error; the error increases with increasing mode number. This error in the phase velocities, or the eigenvalues, can cause substantial shifts in the modal interference pattern. We will shortly see an example of this.

Even with those limitations, however, the parabolic equation model has become an extremely useful tool in electromagnetic and acoustic propagation and is used extensively in both.

We chose 3 GHz so that we could compare our results with EMPE. We needed a test case for comparison because of the major modifications made in the acoustic computer code. The modifications resulted not only from the changes brought about when converting from acoustic wave propagation to electromagnetic wave propagation, but also from converting the code that originally ran on a VAX 11/780 computer to a Cray X-MP/24 computer.

The radio refractivity N is defined by

$$N = (n - 1) \times 10^6 \quad (25)$$

and may be determined empirically at any altitude from knowledge of the atmospheric pressure, the temperature, and the partial pressure of water vapor.

The vertical refractivity profile used for the 3-GHz case is listed below. Figure 3 is a plot of the refractivity.

Height (m)	Refractivity
0	299.997
61	260.014
365.8	247.966

We want to compare the transmission loss calculated by the coupled-mode model with that calculated by EMPE; because EMPE does not handle a rough sea surface, the comparison was done for a flat sea surface. Transmission loss, *TL*, is a measure of the loss in intensity of the electromagnetic wave between a point 1 m from the source and a receiver at some arbitrary distance from the source. If *I*₀ is the intensity at 1 m from the source and *I* is the intensity at the receiver, the transmission loss between the reference distance of 1 m and the distant receiver is

$$TL = 10 \log(I_0/I) \text{ dB} . \quad (26)$$

We see from the vertical refractivity profile that there is a 61-m-high surface duct. At 3 GHz, seven modes are trapped in this duct. They alone would give an adequate description of the transmission loss for a source and receiver located in the duct, provided there was no mechanism, such as a rough surface, to scatter energy out of the duct. There are 29 modes trapped in the 365.8-m waveguide, and we included all of them in our calculations. A trapped mode is a mode having a phase velocity that is realized in the waveguide. We can calculate the

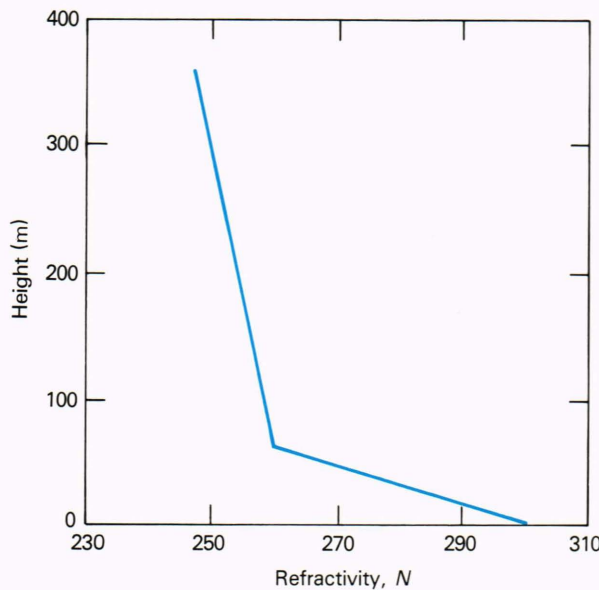


Figure 3—Refractivity versus height for the 3-GHz case.

wave velocity in the waveguide by using Eqs. 25 and 3 and the values of the refractivity found in the text table above. The wave velocity at 0 m is 2.9970259×10^8 m/s, and the wave velocity at 365.8 m is 2.9971818×10^8 m/s. All modes with a phase velocity between these two values (which represent the maximum and minimum values of the velocity in the waveguide) are said to be trapped.

Although the model can accommodate absorption, we have neglected it in all runs. We put the source and receiver in the duct at a height of 15.2 m. The source is an omnidirectional point radiator.

Figure 4 is a comparison of the transmission loss calculated by the coupled mode model with that calculated by EMPE. The comparison is good. We discussed above why the modal interference pattern of EMPE does not agree exactly with the coupled-mode model. Shifts in the interference pattern of EMPE are not a serious limitation. No deterministic model can predict exactly the transmission loss between two fixed points, whether or not the model calculates the eigenvalues correctly. Shifts in the interference pattern do not affect the general propagation characteristics that are produced by a refractivity profile. If one is looking for anomalies in the propagation, such as shadow zones or ducting, they will be there. For most applications it does not matter if the model predicts them to be at a slightly different range than where they were measured. In addition, EMPE has been well validated by comparison with experimental data.

PROPAGATION IN A TROPOSPHERIC DUCT AT 35 GHz

The long-term objective of this project is to investigate the effect of capillary waves on the scattering of mil-

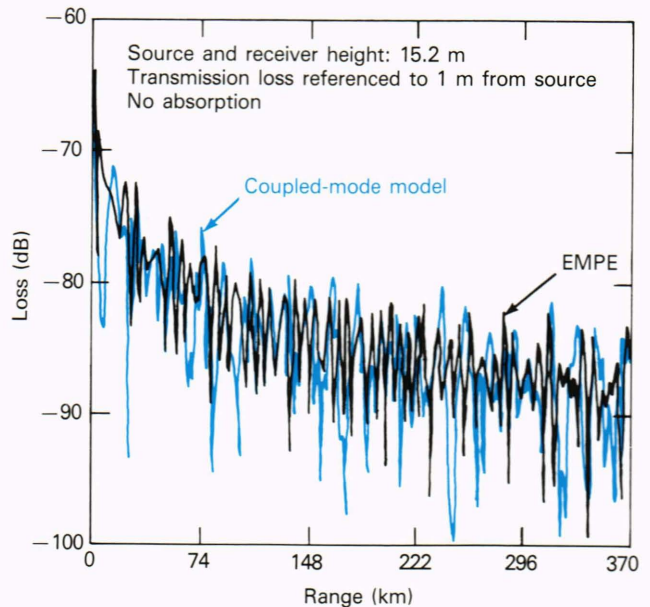


Figure 4—Transmission loss versus range for the 3-GHz case, computed by EMPE and coupled-mode models for a flat sea surface.

limeter electromagnetic waves propagating over long ranges in a tropospheric duct. The first goal was to ascertain whether the acoustic coupled-mode model could even handle the problem. At this point in the investigation, we have just finished answering that question in the affirmative. The examples shown in this section are only meant to demonstrate that millimeter-electromagnetic-wave propagation in a tropospheric duct overlying a rough sea surface can be addressed by the coupled-mode model. We also want to emphasize that the results in this section for rough-surface scattering from capillary waves should not necessarily be taken as correct, because of the current representation of the capillary-wave profile, which is independent of the coupled-mode model. We will have more to say about the problem later.

Now let us discuss propagation at 35 GHz in a tropospheric duct. Table 1 shows the vertical refractivity profile that we used for this case. Figure 5 is a plot of refractivity versus altitude. Figure 6, an enlargement of the first 70 m of the profile, shows that a strong surface duct is present in the first 14 m of altitude.

First, let us calculate transmission loss for a 500-m-high waveguide with a flat sea surface. Since the coupled-mode model uses exactly the same algorithm whether the surface is flat or rough, we can conclude that if it works for a flat surface it will work for a rough surface. There are 493 modes trapped in this waveguide. We put the source at 9.5 m and again we neglect absorption.

Figures 7, 8, and 9 show vertical transmission-loss profiles from 0 to 500 m at ranges of 92.7, 185.3, and 278 km, respectively. One can see how the energy slowly spreads out of the duct over these ranges. At 92.7 km,

the coverage is fairly good up to about 430 m, but there are almost periodic holes in that coverage. When we get to 278 km, there is no coverage above approximately 200 m. Figure 10 shows transmission loss versus range for a receiver also at 9.5 m.

Now let us consider a rough surface. The wavelength of the electromagnetic waves at 35 GHz is 8.6 mm. The

Table 1—Vertical refractivity profile used in the 35-GHz case.

Height (m)	Refractivity, <i>N</i>
0	350.00
1	328.67
2	327.33
3	326.67
4	326.00
5	325.66
6	325.33
7	325.00
8	324.66
9	324.48
10	324.33
12	323.86
14	323.66
16	323.33
32	321.33
50	320.00
70	318.66
100	316.99
200	312.65
500	300.97

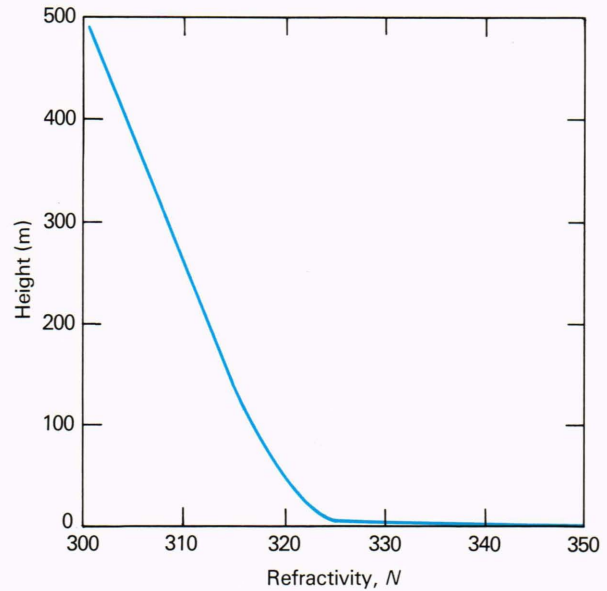


Figure 5—Refractivity versus height for the 35-GHz case.

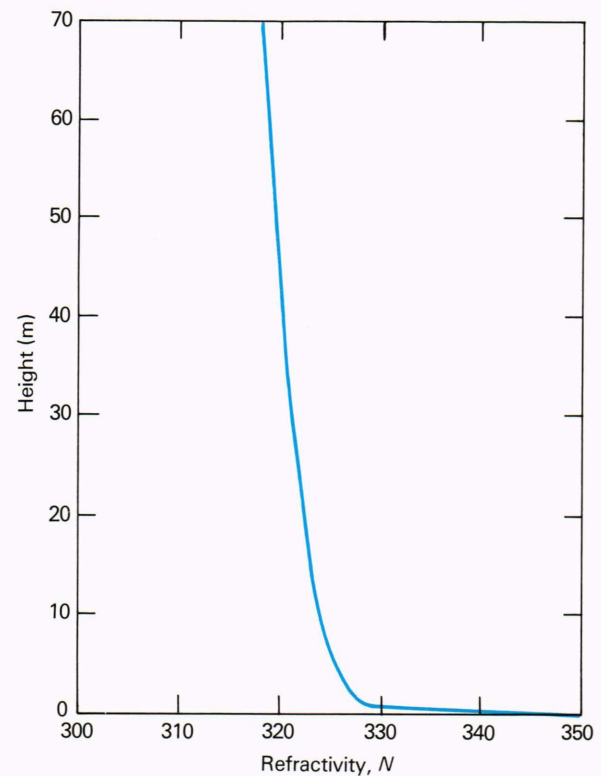


Figure 6—Refractivity profile for the first 70 m of the troposphere for the 35-GHz case.

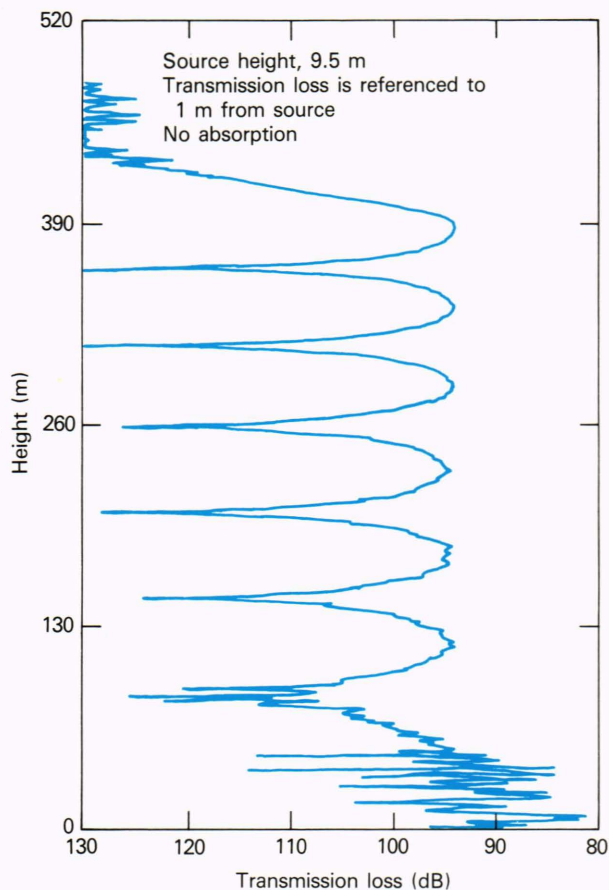


Figure 7—Transmission loss versus height for the 35-GHz case at a range of 92.7 km for a flat sea surface.

water wavelength that gives rise to Bragg scattering is approximately 4.3 mm; that corresponds to a frequency of 80 Hz and is in the capillary regime. Consequently, for a test case we decided to include waves in the frequency range 50 to 80 Hz. We started at 50 Hz because that is approximately the lower limit for capillary waves. In any study of scattering from capillary waves, we would want to include water-wave frequencies at the Pierson-Moskowitz end of the spectrum, so that the capillary waves would be riding on the longer gravity waves.

Even though we believe that we have a suitable spectrum for capillary waves in the Liu-Lin spectrum, there is no reason to believe that Eq. 17 may not be a good representation of the capillary-wave profile. In the Pierson-Moskowitz regime, Eq. 17 is a good representation of the sea surface, especially at low grazing angles. Figure 11 shows a section of a capillary-wave profile calculated from Eq. 17 using the Liu-Lin spectrum for a wind speed of 28 kt. The calculated profile does not have many of the features of a theoretical profile, calculated by Crapper,¹⁷ that represents an exact nonlinear solution. Any future work would have to resolve that problem.

Figure 12 is a comparison of the transmission loss for a flat sea surface with that for the randomly rough capillary-wave surface described above. The integration step

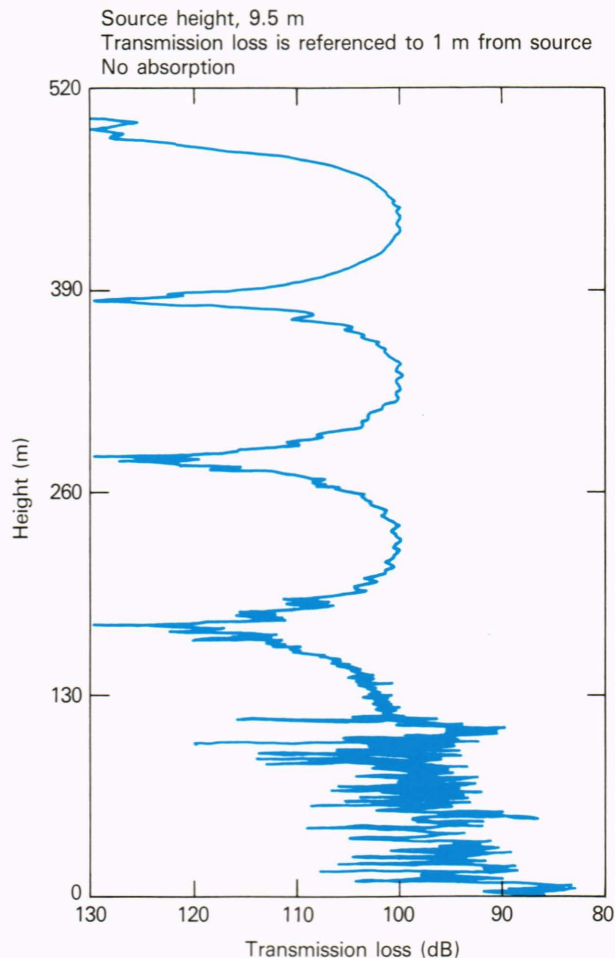


Figure 8—Transmission loss versus height for the 35-GHz case at a range of 185.3 km for a flat sea surface.

size was one-sixteenth that of the smallest water wavelength. No conclusions should be drawn from a comparison of these two curves, for reasons to be discussed in the next section.

CONCLUSIONS AND FUTURE DIRECTIONS

We have demonstrated that an existing acoustic, coupled-mode model can be used to describe millimeter-electromagnetic-wave propagation and scattering in a tropospheric duct overlying a randomly rough sea surface.

Future work will be directed at the following areas:

1. Surface realization model for capillary waves.
2. Boundary condition at the top of the atmosphere.
3. Inclusion of a range-dependent environment.
4. Boundary conditions at the sea surface.

We have already discussed the problems of the surface representation for capillary waves and the boundary condition at the top of the atmosphere. For the cases discussed here, a rigid upper boundary was used with no absorbing layer beneath it. We included only modes that were trapped in the waveguide so that none reflected off the rigid surface. Consequently, if the rough surface used in our example scattered energy into high

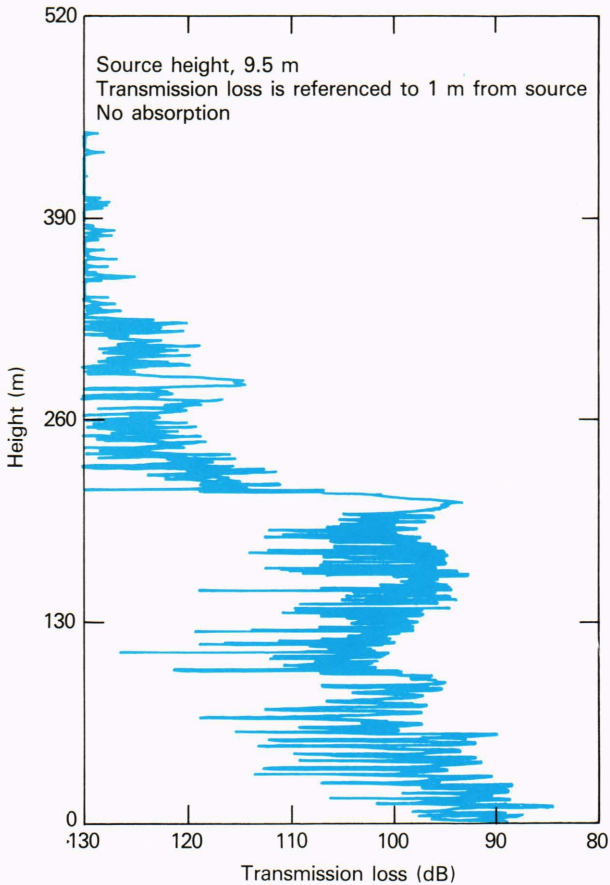


Figure 9—Transmission loss versus height for the 35-GHz case at a range of 278 km for a flat sea surface.

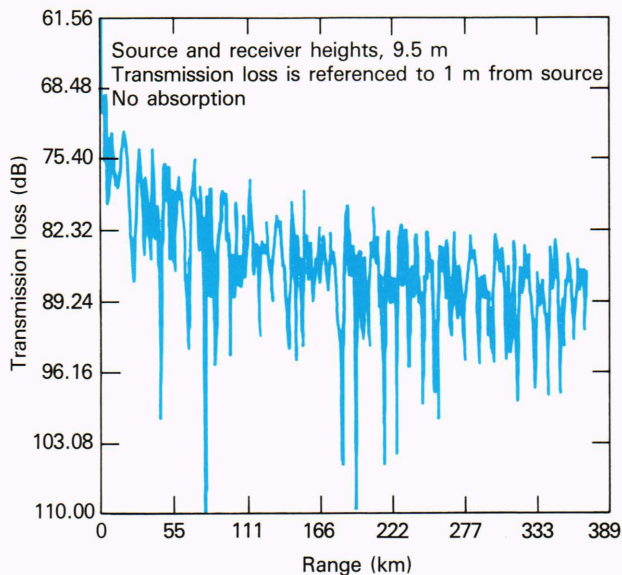


Figure 10—Transmission loss versus range for the 35-GHz case for a flat sea surface.

angles, we may not have had enough of the higher-order modes to correctly account for that scattering. This is another reason that the transmission loss shown in Fig.

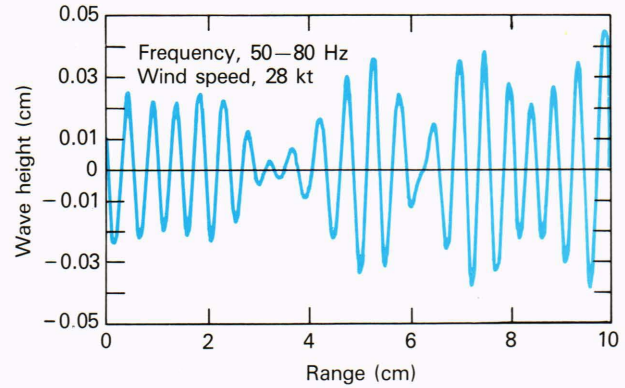


Figure 11—Section of a capillary-wave profile.

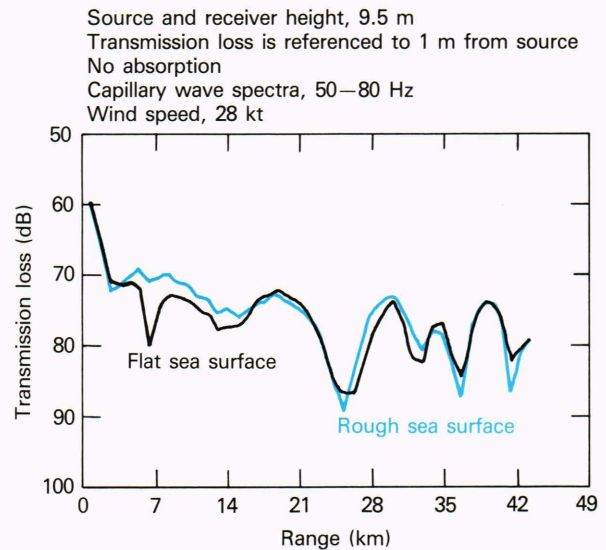


Figure 12—Transmission loss versus range for the 35-GHz case; integration step size is 0.25 mm.

12 may not be exact. Again, the example was only intended as a demonstration that the coupled-mode model would run for the electromagnetic case.

As shown by Eq. 15, the coupled-mode theory allows for a waveguide in which the refractive index varies horizontally as well as vertically. The range-dependent refractive index has not been coded into the computer program, however. Where surface duct thickness varies along the track, it is imperative to account for this variation.

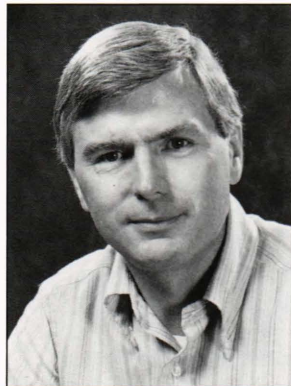
The present model treats only the case of a horizontally polarized electric wave and an infinitely conducting sea. Future work should extend the theory to treat vertical polarization and a sea with finite conductivity.

REFERENCES

- ¹C. A. Boyes, L. B. Dozier, and G. W. Joice, "Application of Coupled Mode Theory to Acoustic Scattering from a Rough Sea Surface Overlaying a Surface Duct," *Johns Hopkins APL Tech. Dig.* **6**, 216–226 (1985).
- ²C. A. Boyes, *Acoustic Waveguides: Applications to Oceanic Science*, Chap. 7, John Wiley and Sons, New York (1984).
- ³L. B. Dozier, "Numerical Solution of Coupled Mode Equations for Rough Surface Scattering," *J. Acoust. Soc. Am.* **73** (Supplementary), S96 (1983).

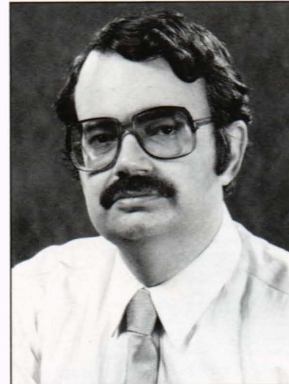
- ⁴P. M. Morse and H. Feshbach, *Methods of Theoretical Physics: Part 1*, Chap. 5, McGraw-Hill, New York (1953).
- ⁵M. Born and J. R. Oppenheimer, "Quantum Theory of Molecules," *Ann. Phys. (Leipzig)* **84**, Ser. 4, 457-484 (1927).
- ⁶D. Marcuse, *Theory of Dielectric Optical Waveguides*, Chap. 3, Academic Press, New York (1974).
- ⁷L. Fortuin, "The Wave Equation in a Medium with a Time-Dependent Boundary," *J. Acoust. Soc. Am.* **53**, 1683-1685 (1973).
- ⁸F. M. Labianca and E. Y. Harper, "Connection Between Various Small-Waveheight Solutions of the Problem of Scattering from the Ocean Surface," *J. Acoust. Soc. Am.* **62**, 1144-1157 (1977).
- ⁹C. A. Boyles, *Acoustic Waveguides: Applications to Oceanic Science*, Chap. 5, John Wiley and Sons, New York, pp. 197-201 (1984).
- ¹⁰E. Y. Harper and F. M. Labianca, "Perturbation Theory for Scattering of Sound from a Point Source by a Rough Surface in the Presence of Refraction," *J. Acoust. Soc. Am.* **57**, 1044-1051 (1975).
- ¹¹B. Kinsman, *Wind Waves*, Chap. 8, Prentice-Hall, Englewood Cliffs, N.J. (1965).
- ¹²W. J. Pierson, Jr., and L. Moskowitz, "A Proposed Spectral Form for Fully Developed Wind Seas Based on the Similarity Theory of S. A. Kitaigorodskii," *J. Geophys. Res.* **69**, 5181-5190 (1964).
- ¹³H. Liu and J. Lin, "On the Spectra of High Frequency Wind Waves," *J. Fluid Mech.* **123**, 165-185 (1982).
- ¹⁴H. W. Ko, J. W. Sari, and J. P. Skura, "Anomalous Microwave Propagation Through Atmospheric Ducts," *Johns Hopkins APL Tech. Dig.* **4**, 12-26 (1983).
- ¹⁵R. M. Fitzgerald, "Helmholtz Equation as an Initial Value Problem with Applications to Acoustic Propagation," *J. Acoust. Soc. Am.* **57**, 839-842 (1975).
- ¹⁶S. T. McDaniel, "Propagation of Normal Mode in the Parabolic Approximation," *J. Acoust. Soc. Am.* **57**, 307-311 (1975).
- ¹⁷G. D. Crapper, "An Exact Solution for Progressive Capillary Waves of Arbitrary Amplitude," *J. Fluid Mech.* **2**, 532-540 (1957).

THE AUTHORS



C. ALLAN BOYLES holds B.S. and M.S. degrees in physics from the Pennsylvania State University and has completed the course work and partial thesis work for a Ph.D. He worked in underwater acoustics at the Ordnance Research Laboratory at Penn State from 1964 to 1967 and at TRACOR from 1967 to 1970. He joined APL's Submarine Technology Department in 1970. From 1970 to 1981, Mr. Boyles developed the theory of acoustic Luneburg lenses and helped design, conduct, and analyze sea tests to measure signal transmission and coherence and ambient noise in the

ocean. Since 1981, his main effort has been in developing the mathematical theory of acoustic wave propagation in the ocean, with emphasis on rough surface scattering. He is author of the book, *Acoustic Waveguides: Applications to Oceanic Science*. He is a member of the Principal Professional Staff and is Supervisor of the Propagation and Noise Analysis Section.



LEWIS B. DOZIER is a senior applied mathematician at Science Applications International Corp. (SAIC), McLean, Va., specializing in the modeling of underwater acoustic propagation. He was born in Rocky Mount, N.C., in 1947. After receiving his B.S. in mathematics from Duke in 1969, he joined the Bell Telephone Laboratories, where he was involved in the development of large-scale computer simulations of magnetohydrodynamics, with applications to advanced ballistic missile defense systems. Meanwhile, he earned his M.S. in mathematics from the Courant Institute of New York

University in 1972. In 1973, he became involved with ocean acoustics and was responsible for designing the logic of a computer simulation to evaluate system performance. In 1974, Mr. Dozier left Bell Laboratories to do doctoral research at the Courant Institute.

In 1977, he joined the staff of SAIC, where he has continued to pursue his interest in acoustic fluctuations due to the random ocean medium and boundaries. He has been principal investigator of several research efforts in that field, including considerable collaboration with APL. A novel technique for numerical computation of scattering from a rough ocean surface was published in 1984.